

## Spin dynamics of Gd in an applied magnetic field

This article has been downloaded from IOPscience. Please scroll down to see the full text article.

1989 J. Phys.: Condens. Matter 1 7425

(<http://iopscience.iop.org/0953-8984/1/40/016>)

View [the table of contents for this issue](#), or go to the [journal homepage](#) for more

Download details:

IP Address: 171.66.16.96

The article was downloaded on 10/05/2010 at 20:25

Please note that [terms and conditions apply](#).

## Spin dynamics of Gd in an applied magnetic field

J W Cable and R M Nicklow

Oak Ridge National Laboratory, Solid State Division, PO Box 2008, Oak Ridge,  
TN 37831-6393, USA

Received 8 March 1989

**Abstract.** Quasi-elastic and inelastic neutron scattering were used to study the effect of an applied magnetic field on the spin dynamics of Gd at temperatures near  $T_c$ . The quasi-elastic critical scattering shows a rapid decrease with applied field which is well reproduced by an RPA model. At these elevated temperatures the spin wave energies are proportional to the magnetisation only at small  $q$ . At larger  $q$ , they shift upward in accordance with the correlation theory treatment by Lindgård. In both wavevector regions, the spin wave spectra are the same at equivalent magnetisations, regardless of whether that is a spontaneous magnetisation at  $T < T_c$  or an induced magnetisation at  $T > T_c$ .

### 1. Introduction

In this paper, we report a neutron study of the effect of an applied magnetic field on the spin dynamics of Gd. In this predominantly Heisenberg ferromagnet, the spin at a given lattice site experiences an effective molecular field comprised of the near-neighbour exchange field plus the applied field. At temperatures near  $T_c$ , even small applied fields will dramatically alter both the order parameter,  $\langle S^z \rangle$ , and the spin-pair correlations,  $\langle S_i^\alpha S_j^\alpha \rangle - \langle S_i^\alpha \rangle \langle S_j^\alpha \rangle$ . Several years ago, Villain [1] calculated the field and temperature dependences of these spin-pair correlations using the RPA along with the Landau model for the moment fluctuations. He obtained transverse and longitudinal susceptibilities of the Van Hove [2] form,  $\chi_q = [r_1^2(\kappa_1^2 + q^2)]^{-1}$ , for which both  $r_1^2$  and  $\kappa_1^2$  are field and temperature dependent. The results, which are valid for small  $q$ , are in excellent agreement with early neutron measurements [3] of the field-dependent critical scattering from Fe. More recently, the spin correlations at general  $q$  and  $T$  were treated by Lindgård [4] using both the RPA and a correlation theory which takes spin-wave interactions and damping into account by use of a mode-mode coupling approximation. In the present experiment, we investigate the field dependence of the quasi-elastic and inelastic magnetic scattering near  $T_c$ . We first examine the quasi-elastic critical scattering near (110) and compare the results with the RPA calculation by Villain [1]. We then observe the field dependence of the inelastic scattering at  $Q = (0, 0, 2 - \zeta)$  for small and intermediate  $\zeta$ -values. These results are compared with the correlation theory calculation by Lindgård [4].

### 2. Experimental results

The neutron measurements were made on a single crystal of  $^{160}\text{Gd}$  with a volume of about  $3 \text{ cm}^3$  and a mosaic spread of about  $20'$ . For the critical scattering measurements,

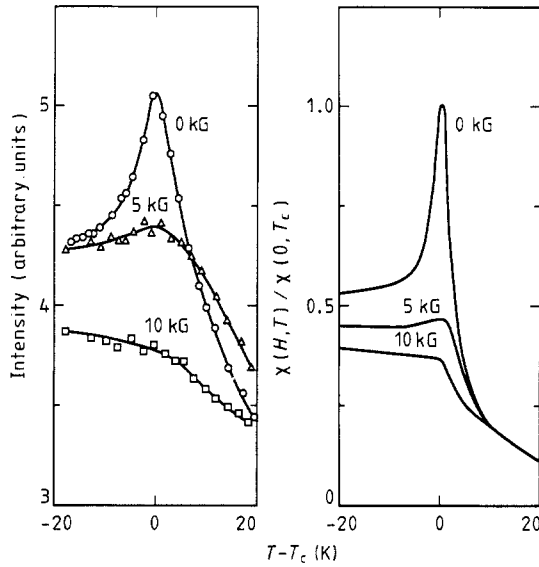


**Figure 1.** Comparison of the critical scattering intensity from Gd ( $T_c = 293$  K) with an RPA calculation of  $\chi(H, T)$  following Villain [1]. The scale offset on the left removes a large, nuclear-scattering contribution and thereby emphasises the magnetic scattering.

the crystal was mounted with the  $c$  axis vertical and the magnetic field was applied to this  $\langle 001 \rangle$  direction. The intensity at  $Q = (1 - \delta, 1 - \delta, 0)$  with  $\delta = 0.025$  was taken as a function of temperature in a constant magnetic field. Some of the results are presented in figure 1 which shows raw intensity data taken in 2-axis geometry with an incident energy of 35 meV. It should be noted that these data include a large, temperature-independent contribution from the nuclear scattering at the foot of the  $(110)$  Bragg peak. The intensity scale in figure 1 has been offset to partially negate this nuclear scattering and to emphasise the magnetic scattering component. It should also be noted that absolute intensities are extremely sensitive to crystal rotation angles at settings this close to the Bragg peak. Here, the  $H = 0$  and  $H = 10$  kG data were taken at one setting of the crystal, while crystal rotation and repositioning occurred before the  $H = 5$  kG data were taken. It is quite likely that the apparent crossing of the  $H = 0$  and  $H = 5$  kG data is simply an artefact arising from a small repositioning error. The theory [1] suggests that the intensities at all three field conditions should merge above  $T_c$ .

Under the conditions of this experiment, the detector effectively integrates over energy at constant  $q$ , and the observed magnetic scattering is simply proportional to the generalised susceptibility,  $\chi_q$ . With  $H$  parallel to  $\langle 001 \rangle$  and  $Q$  parallel to  $\langle 110 \rangle$  the observed  $\chi_q$  is the sum of susceptibilities parallel and perpendicular to the applied field direction. According to Villain [1], these are given by

$$\chi_q^{\parallel} = (dH/dM + Aq^2)^{-1} \quad (1)$$

and

$$\chi_q^{\perp} = (H/M + Aq^2)^{-1} \quad (2)$$

where  $A = 2Ja^2/g^2\mu^2$ . Here,  $J$  is the exchange constant,  $a$  is the lattice constant, and the  $M(H)$  dependence must be taken from an appropriate model. Villain uses the Landau model for  $M(H)$  and obtains analytical expressions for  $\chi_q^{\parallel}$  and  $\chi_q^{\perp}$ . The  $\chi(H, T)/\chi(0, T_c)$

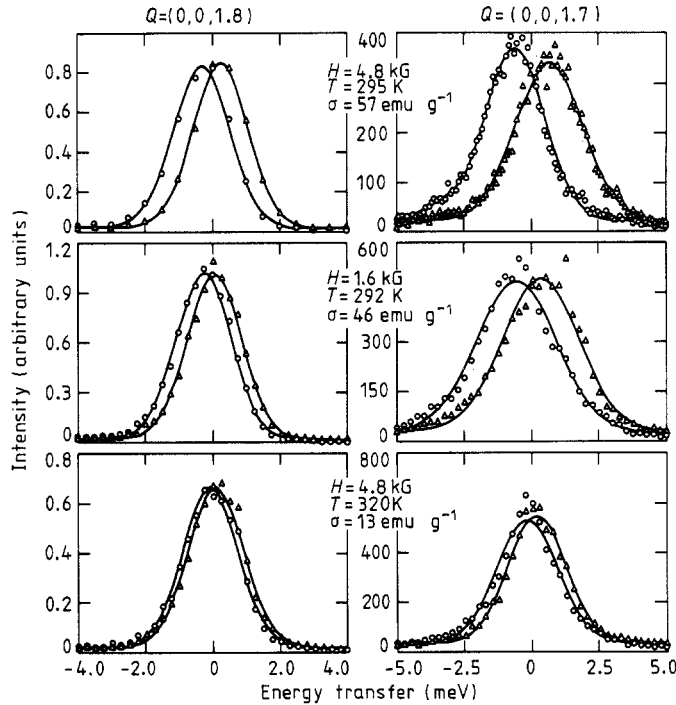


**Figure 2.** Polarised-neutron, magnetic-excitation spectra of Gd in forbidden magnon geometry with  $H \parallel Q$ . The open triangles correspond to flipper-off data and spin-wave-creation spectra, while the open circles represent flipper-on data and spin-wave-annihilation spectra.

ratios shown on the right-hand side of figure 1 were calculated from these expressions using known parameters for Gd. Here,  $\chi(H, T) = \chi^{\parallel}(H, T) + \chi^{\perp}(H, T)$  in accordance with the experimental geometry. Clearly, this RPA treatment provides a reasonable description of the observed  $\chi(H, T)$ . The calculated functions are sharper in  $T$ , but this difference may be associated with the  $q$ -resolution of the spectrometer. The dramatic suppression of the critical scattering by an applied field is certainly well reproduced.

The data shown in figure 1 correspond to equal-time, spin-pair correlations in the limit of small  $q$ . Inelastic neutron scattering measurements are required to go beyond these limits and investigate the field dependence of the dynamic response of the spin system. For these measurements, the crystal was reoriented with a  $\langle 110 \rangle$  axis vertical and the magnetic field was applied parallel to the scattering vector in an  $\langle 001 \rangle$  direction. Triple-axis data were taken at a fixed incident energy of 40 meV using an  $^{57}\text{FeSi}$  monochromator to produce a polarised neutron beam. The polarisation was maintained alternately parallel and antiparallel to both  $Q$  and  $H$  by means of a neutron spin flipper located between the monochromator and the sample. Under these experimental conditions, spin wave creation occurs only for neutrons with spins antiparallel to the sample spins. Likewise, spin wave annihilation occurs only for neutrons with parallel spins [5, 6]. This complete separation of the energy-loss and energy-gain spectra according to incident neutron spin state allows the determination of the peak positions at energies much smaller than the energy resolution of the spectrometer. Typical results are given in figure 2 which shows energy spectra for the two spin states at  $Q = \langle 0, 0, 2 - \zeta \rangle$

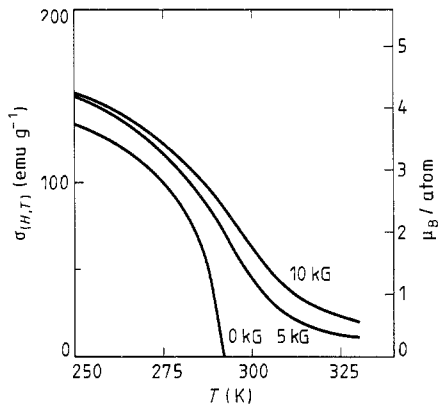


**Figure 3.** Magnetisation of Gd in the  $\langle 00l \rangle$  direction [7].

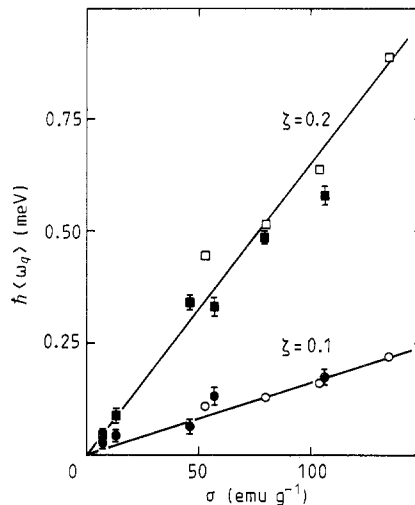


**Figure 4.** Spin wave energy of Gd versus magnetisation. The full points represent the present results taken in an applied field, while the open points refer to zero-field data at  $T < T_c$  [8].

for  $\zeta = 0.2$  and  $0.3$  under various conditions of  $H$  and  $T$ . The flipper-off data (open triangles), correspond to the energy-loss or spin-wave-creation spectra while the flipper-on data (open circles) represent the energy-gain or spin-wave-annihilation spectra. The observed spectra were corrected for polarising deficiencies of the spectrometer and for depolarisation in the sample before fitting to a constant background plus a Gaussian peak. With the spin wave energy defined as one-half the separation of the flipper-off and the flipper-on peaks, we are able to determine spin wave energies down to  $0.03$  meV even though the elastic energy resolution of the spectrometer is  $1.6$  meV (FWHM). As expected, the spectra in figure 2 show an increase in the spin wave energies with both  $\zeta$  and the magnetisation,  $\sigma$ . Here, and throughout the remainder of this paper, the magnetisation values are taken from [7] whose data in the  $H$  and  $T$  range relevant to this experiment are shown in figure 3. These data, taken for magnetisation along the  $c$  axis, show large field effects on the order parameter with the largest effects occurring at  $T_c$ . The  $\zeta = 0.1$  and  $0.2$  data are summarised in figure 4 which shows the spin wave energies as a function of the magnetisation. The full data points represent the present results in an applied field and the open data points are from previous measurements [8] in zero field but at temperatures below  $T_c$ . Within experimental error the spin wave energies are directly proportional to the magnetisation whether spontaneous or induced. This is the expected result at small  $q$  where the damping remains small and spin wave peaks with energies of  $\hbar \langle \omega_q \rangle$  remain observable up to  $T \approx T_c$ . Typical results at larger  $q$  are given in figure 5 which shows spin wave creation spectra at  $\zeta = 0.5$ . The full data points are current results taken at  $Q = (0, 0, 1.5)$  in an applied field of  $4.8$  kG and at  $T = 295$  K. The induced magnetisation for these  $H$  and  $T$  conditions is  $57$  emu  $g^{-1}$ . The open data points were taken at  $Q = (0, 0, 2.5)$  in zero field and at  $T = 287$  K where the spontaneous magnetisation is  $53$  emu  $g^{-1}$ . The two data sets are approximately normalised at the peak position. They are clearly the same within experimental error.

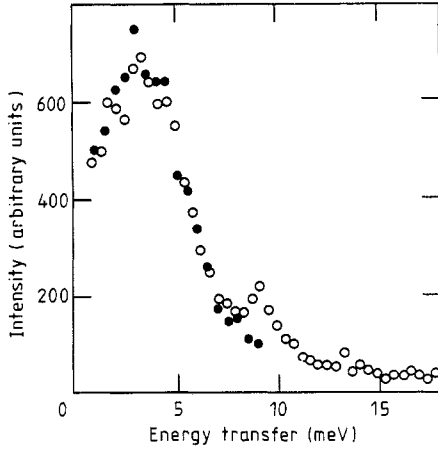


**Figure 5.** Comparison of the magnetic excitation spectra of Gd at  $Q = 0, 0, 2 \pm \zeta$  under  $H$  and  $T$  conditions that produce nearly equivalent spontaneous and induced magnetisations.

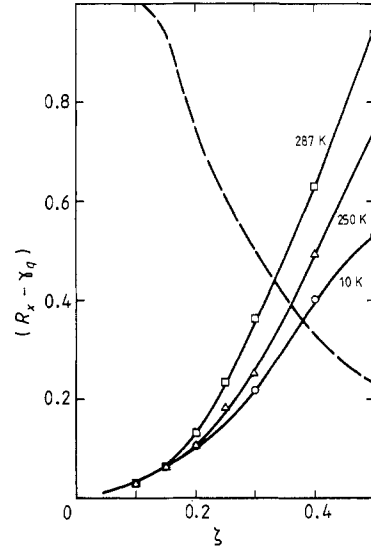


**Figure 6.** The  $\zeta$ -dependence of  $\langle \omega_q \rangle (J_0 M)^{-1} = (R_x - \gamma_q)$  for Gd ( $Q = 0, 0, 2 \pm \zeta$ ) at three selected temperatures. The broken curve shows the  $\zeta$ -dependence at  $T = 287$  K of the prefactor  $[2 - (R_x - \gamma_q)/(1 - \gamma_q)]$  which appears in the  $H$ -dependent term of equation (5).

In this experiment for which  $Q$  and  $H$  are parallel to the  $\langle 001 \rangle$  direction, only the transverse response is observed. According to Lindgård [4], the first frequency moment is then

$$\langle \omega_q \rangle = M / \chi_q^t \quad (3)$$

where

$$\chi_q^t = \frac{1}{J_0} \frac{M^2(h - \gamma_q) + b'_x(1 - \gamma_q)}{M^2(h - \gamma_q)^2 + (a_x - \gamma_q b'_x)(1 - \gamma_q)}. \quad (4)$$

Here,  $M = 2\langle S^2 \rangle$  is the magnetisation and  $h = 1 + H/J_0M$  is the effective molecular field in units of the exchange field.  $\gamma_q$  is defined by the expression  $J_q = J_0\gamma_q$  while  $a_x$  and  $b'_x$  represent local correlations of the spin fluctuations away from long-range order. These correlations can be calculated to self consistency by an iterative procedure but here we take the experimental approach and extract the effects of correlation from the observed spin wave data. We first estimate the magnitude of  $H/J_0M$  from the mean field expression  $k_B T_c = \frac{2}{3} J_0 S(S+1)$ , where  $T_c = 293$  K for Gd. This yields  $J_0M = 16.8 \sigma/\sigma_0$  meV (where  $\sigma/\sigma_0$  is the relative magnetisation) to be compared with the applied field  $g\mu H = 0.012$  meV  $\text{kG}^{-1}$ . Thus,  $H/J_0M$  is always a small number under the conditions of this experiment and equation (4) can then be expanded in  $H/J_0M$ . To first order, the inverse susceptibility becomes

$$\frac{1}{\chi_q^t} = J_0(R_x - \gamma_q) + \left(2 - \frac{R_x - \gamma_q}{1 - \gamma_q}\right) \left(\frac{M}{M^2 + b'_x}\right) H \quad (5)$$

where

$$R_x = (M^2 + a_x)/(M^2 + b'_x). \quad (6)$$

These expressions for the susceptibility are valid at temperatures both above and below  $T_c$ . For  $T \ll T_c$ , where  $M^2 \gg a_x$  (or  $b'_x$ ) and  $R_x \rightarrow 1$ , equation (5) assumes the RPA form and  $\hbar\langle\omega_q\rangle$  corresponds to the spin wave energy. At elevated temperatures the dynamical response becomes more complicated. Spin wave annihilation now occurs, and this produces neutron energy gain peaks so that  $\langle\omega_q\rangle$  tends toward zero. Also, spin wave interactions lead to broadening of the spin wave peaks, and this becomes more severe with increasing  $q$  and  $T$ . Under these conditions, the meaning of  $\langle\omega_q\rangle$  becomes somewhat obscure since the  $\langle\omega_q\rangle$  values obtained by fitting the experimental data depend on the particular spectral weight function used in the fitting. In our previous study of Gd [8], the data were fitted with a damped harmonic oscillator (DHO) function, the shape of which is defined by the second frequency moment,  $\langle\omega_q^2\rangle$ , and a damping parameter,  $\beta_q$ . In the following, we equate the peak position of this DHO function with the spin wave energy; this is given by  $\omega_{\text{peak}} = (\langle\omega_q^2\rangle - 2\beta_q^2)^{1/2}$ . The importance of the correlation effects denoted by  $a_x$  and  $b'_x$  in equation (6) is illustrated by figure 6 which shows the  $\xi$ -dependence of  $(R_x - \gamma_q)$  for Gd at  $Q = (0, 0, 2 \pm \xi)$  for a few selected temperatures. Here,  $(R_x - \gamma_q)$  was calculated from equations (3) and (5) with  $\langle\omega_q\rangle \equiv \omega_{\text{peak}}$  taken from our previous zero-field measurements [8] on Gd. At  $T = 10$  K, the correlation effects are unimportant and the data points correspond to  $(1 - \gamma_q)$  values. The departure of the other data points from  $(1 - \gamma_q)$  as  $T$  approaches  $T_c$  shows the importance of the correlation effects for the spin dynamics of this system. At small  $\xi$ ,  $R_x \approx 1$  and  $\langle\omega_q\rangle$  should remain proportional to  $M$  even as  $T$  approaches  $T_c$ . This is consistent with the  $\langle\omega_q\rangle$ -versus  $-\sigma$  dependence shown in figure 4. However,  $R_x - 1$  increases with both  $T$  and  $\xi$  so  $\langle\omega_q\rangle$  is no longer proportional to  $M$  at intermediate  $T$  and  $\xi$  values. An interesting result of this  $(R_x - \gamma_q)$  behaviour is that the prefactor  $[2 - (R_x - \gamma_q)/(1 - \gamma_q)]$  to the field-dependent term in equation (5) decreases with increasing  $\xi$  and  $T$ . The broken curve in figure 6 shows the  $\xi$ -dependence of this prefactor at  $T = 287$  K. Clearly, any effect of an applied field on the spin wave energies tends to be cancelled by the correlations at intermediate  $\xi$ -values.

In summary, we have observed the critical and inelastic neutron scattering from Gd in applied magnetic fields and at temperatures near  $T_c$ . The critical scattering is strongly suppressed by an applied field, and this suppression is reasonably well explained by the RPA and Landau model treatment by Villain. At these elevated temperatures, the spin wave energies are proportional to the magnetisation, as in linear-spin-wave theory, only at small  $q$ . At larger wavevectors, these energies shift upward due to correlation effects and are no longer directly proportional to the magnetisation. This behaviour is consistent with the correlation theory treatment by Lindgård. Comparison of the spin wave spectra obtained in an applied field with previous zero-field data shows that the spectra are the same for  $H$  and  $T$  conditions that produce the same magnetisations, whether induced or spontaneous.

### Acknowledgments

The authors are indebted to T L Collins and J R Weir III for technical assistance. This research was supported by the Division of Materials Sciences, US Department of Energy under Contract No DE-AC05-84OR21400 with Martin Marietta Energy Systems, Inc.

**References**

- [1] Villain J 1963 *J. Physique* **24** 622
- [2] Van Hove L 1954 *Phys. Rev.* **95** 1374
- [3] Jacrot B, Konstantinovic J, Parette G and Cribier D 1963 *Inelastic Scattering of Neutrons in Solids and Liquids* vol II (Vienna: IAEA) p 317
- [4] Lindgård P A 1984 *Phys. Rev. B* **30** 2729
- [5] Saenz A W 1960 *Phys. Rev.* **119** 1542
- [6] Sokoloff J B 1975 *J. Phys. F: Met. Phys.* **5** 1946
- [7] Nigh H E, Legvold S and Spedding F H 1963 *Phys. Rev.* **132** 1092
- [8] Cable J W, Nicklow R M and Wakabayashi N 1985 *Phys. Rev. B* **32** 1710